Stability of ex situ biological methanation of H2/CO2 with a mixed microbial culture in a pilot scale bubble column reactor

Laguillaumie Léa, Rafrafi Yan, Moya-Leclair Elisabeth, Delagnes Delphine, Dubos Simon, Spérandio Mathieu, Paul Etienne, Claire Dumas

Title:

Stability of *ex situ* biological methanation of H_2/CO_2 with a mixed microbial culture in a pilot scale bubble column reactor

Authors:

Laguillaumie Léa, Rafrafi Yan, Moya-Leclair Elisabeth, Delagnes Delphine, Dubos Simon, Spérandio Mathieu, Paul Etienne, Dumas Claire*

Affiliations

TBI, Université de Toulouse, CNRS, INRAE, INSA, Toulouse, France

* cl_dumas@insa-toulouse.fr

Abstract:

Biological methanation is a promising technology for gas and carbon valorisation. Therefore, process stability is required to allow its scale up and development. A pilot scale bubble column reactor was used for *ex situ* biological methanation with Mixed Microbial Culture (MMC). A 16S rRNA high throughput sequencing analysis revealed the MMC reached a stable composition with 50-60% *Methanobacterium* in closed liquid mode, a robust genus adapted to large scale constraints. Class *MBA03* was identified as an indicator of process stability. Methanogenic genera moved toward 50% of *Methanothermobacter* when intensifying the process, and proteolytic activity was identified while 94% of H_2/CO_2 was converted into methane at $4NL.L^{-1}.d^{-1}$. This study gives clarifications on the origin of VFA apparitions. Acetate and propionate accumulated when methanogenic activity

weakened due to nutritive deficiency, and when P_{H2} reached 0.7bar. The MMC withstood a storage period of 34d at room temperature indicating its suitability for industrial constraints.

Keywords: CO_2 utilisation; methane; gases fermentation; chemolithoautotrophs; microbial competition; acetate; homoacetogenesis; propionate; biotechnology

Graphical abstract

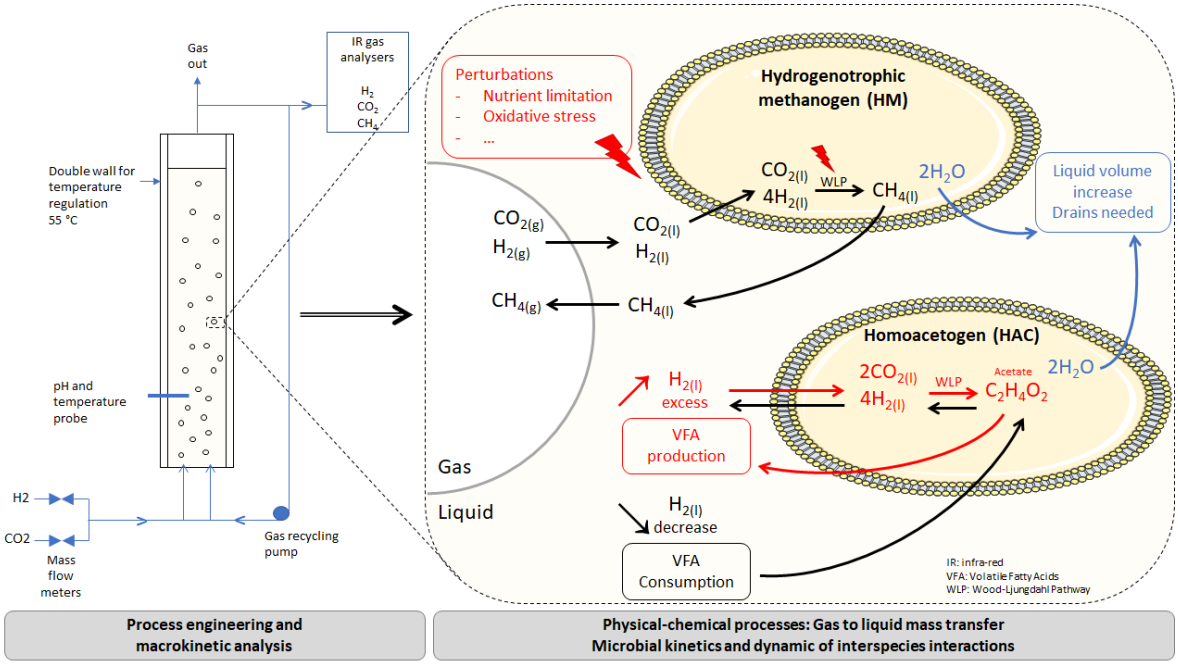

Colour print is needed

High quality file has been provided separately

1. Introduction

Anaerobic biological processes are more and more implemented for organic waste recovery. They enable the production of value-added products, especially methane (CH_4) and hydrogen (H_2) for the production of energy from biomass and organic wastes. These technologies are of great interest in the framework of Green House Gas (GHG) emissions reduction, and to meet the goal of net zero emission by 2050. Biogas produced by anaerobic digestion (AD) contains between 50 % to 70 % of methane and between 30 % and 50 % of carbon dioxide (CO_2) (Angelidaki et al., 2018). Thus, its calorific value is not as high as that of natural gas, and it is important either to separate the CH_4 from the CO_2, or to upgrade the biogas to higher concentrations of methane before injecting it into the gas grid. Biological methanation is an appealing way of upgrading biogas, because the process is quite similar to AD and can be integrated into the biogas production plant. The principle is to convert residual CO_2 with extra H_2 addition through reaction (1) to produce methane. Two processes are developed for biological methanation. The *in situ* processes consist in injecting external H_2 directly in AD reactors. However, H_2 excess in an AD reactor 1) may slow down the first reactions of hydrolysis, acidogenesis and acetogenesis, since the Gibbs free energy (ΔrG) of these hydrogenogenic reactions will increase; 2) may stimulate homoacetogenesis (Grimalt-Alemany et al., 2019; Agneessens et al., 2018; González-Cabaleiro et al., 2013; McCarty and Bae, 2011; Batstone et al., 2002). During *in situ* biological methanation, H_2 supply is therefore a crucial step, and the operating range of process parameters such as temperature, pH, organic and hydraulic loading rates, is narrow to support growth of all the synergistic activities and promote methanogenesis. Conversely, *ex situ* biological methanation requires a second reactor to treat biogas externally to AD reactors. *Ex situ* biological methanation promotes the advantage of being operated under

specific conditions favouring reaction (1), without disturbing the stability of AD, and with the possibility of injecting other CO_2 sources as substrate (Rafrafi et al., 2020; Kougias et al., 2017; Burkhardt et al., 2015; Drosg, 2013). Nevertheless, more operational data of *ex situ* biological methanation pilot scale processes are needed. In particular, with emphasis on process stability and reliability in the face of gas load variations and shutdown periods during long-term operation. This kind of studies will allow to have a certain hindsight to better implement industrial biological methanation systems. Additionally, microbial mixed cultures (MMC) are often used as catalyst of the reaction. Because they can be originated from the AD, they are not expensive and available in AD plants. MMC also do not require sterile conditions, and can withstand process troubles, or operational changes due to the high microbial diversity they contain. Biological interactions within the MMC are of great importance to ensure the stability of the process. Yet, the relation between process stability and MMC composition in the framework of biological methanation has not been well established, even though more and more microbial analysis are undertaken and some effort is made in this direction in the anaerobic digestion field (Campanaro et al., 2020).

Within *ex situ* biological methanation processes, H_2/CO_2 can be directly converted into methane through hydrogenotrophic methanogenesis (HM) according to reaction (1), but also into acetate through homoacetogenesis (HA) according to reaction (2). Once acetate is produced, it can be further converted into methane through acetoclastic methanogenesis (AM) according to reaction (3), or oxidized through syntrophic acetate oxidation (SAO) according to reaction (4), that is reverse reaction (2).

(1) $4H_2 + CO_2 \rightarrow CH_4 + 2H_2O$ ($\Delta G°' = -131$ kJ.mol^{-1}) HM

(2) $4H_2 + 2CO_2 \rightarrow C_2H_4O_2 + 2H_2O$ ($\Delta G°' = -82$ kJ.mol^{-1}) HA

(3) $C_2H_4O_2 \rightarrow CH_4 + CO_2$ ($\Delta G°' = -49$ kJ.mol^{-1}) AM

(4) $C_2H_4O_2 + 2H_2O \rightarrow 4H_2 + 2CO_2$ ($\Delta G°' = +82$ kJ.mol^{-1}) SAO

These reactions i) are carried out by different microorganisms with proper kinetics and optimal conditions ii) operate close to thermodynamic equilibrium, which implies considering the reaction feasibility under given conditions. In the MMC, HM will compete with HA for the same substrate H_2/CO_2 and AM will compete with SAO for acetate, if produced. Maximal specific growth rates of thermophilic HM is higher compared to mesophilic ones (Bassani et al., 2015). Moreover, there is less microbial diversity under thermophilic than under mesophilic temperatures (Grimalt-Alemany et al., 2019). For these reasons, biological methanation is often more efficient under thermophilic than mesophilic conditions when working with MMC (Strübing et al., 2019; Kougias et al., 2017). HA have higher minimal H_2 fixation thresholds than HM (Weijma et al., 2002). Therefore, if H_2 is limiting, and HM active, HA cannot fix H_2, which is maintained at very low thresholds by HM, especially under thermophilic conditions (Pan et al., 2021; Cord-Ruwisch et al., 1988). The use of MMC to carry out biological methanation is hence relevant, because the competitive side reactions are prevented by HM activity, and opportunistic heterotrophs still remain on lysis products, contributing to the durability of the process. This by recycling growth factors, and preventing from toxic accumulations.

In this study, a pilot scale bubble column reactor has been operated for *ex situ* biological methanation of H_2/CO_2 at 55 °C with a MMC. The aim of this study was to investigate the reactivity of the biological methanation process in a dynamic operation mode such as gas load variations, feed intermittence, and to highlight the impact of nutrient limitations on the process performances. This study provides a wide discussion about the process features that

allow to orient the MMC toward the selective and stable methane production regarding different aspects such as nutrient regulation, gas load management and MMC storage conditions. Moreover, it gives some clarifications on the origin of potential VFA accumulations that could compromise methane production.

2. Materials and Methods

2.1 Pilot-scale methanation process

Experiment was carried out in a 22 L bubble column reactor (BCR) of height and internal diameter of 1.200 m and 0.145 m respectively. E*x situ* biological methanation at 55 °C was carried out with synthetic CO_2 as the sole carbon source and synthetic H_2 as electron donor. The reactor was conducted in closed mode for liquid, although some supernatant was replaced by nutrients stock solutions at some periods along the operation to support growth and maintain a constant liquid volume in the reactor by removing volume corresponding to water production of reaction (1). Effective liquid volume was 20 L during periods 1 and 2 and 18 L during period 3. Gas was continuously sparged from the bottom of the column through four porous sintered of 10 mm diameter and porosity between 100 and 160 µm during period 1 and 2. During period 3, a single porous sintered with same properties but 150 mm diameter was implemented, occupying the whole bottom of the column, in order to improve the gas to liquid mass transfer. Gases were supplied from pressurized gas cylinders of H_2 and CO_2 through flow controllers (EL-FLOW® Select F-201CV, Bronkhorst). The gas from the headspace was recirculated at 120 $NL.L^{-1}.d^{-1}$ through a valve pump (Type R 1C 225 H1B, Sirem). Outlet flow was measured with a volumetric gas meter (Ritter®). Temperature was regulated at 55 °C with a thermostat (LAUDA®) circulating water in the

129 double wall of the BCR. Probes for pH (InPro 3100(i) SG 120, Mettler Toledo®), ORP
130 (Polilyte Plus ORP Arc 225, Hamilton™), dissolved CO_2 (InPro 5000(i), Mettler Toledo®)
131 were installed to measure continuously the values of these parameters.
132 Culture medium was composed of NH_4Cl 1 $g.L^{-1}$; KH_2PO_4 0.5 $g.L^{-1}$; $MgCl_2$, $6H_2O$ 0.1 $g.L^{-1}$;
133 $CaCl_2$, $2H_2O$ 0.05 $g.L^{-1}$; Na_2SO_4 0.1 $g.L^{-1}$; $NaHCO_3$ 0.13 $g.L^{-1}$; Na_2S, $9H_2O$ 2 $g.L^{-1}$.
134 Phosphate buffer was also used (K_2HPO_4 2.05 $g.L^{-1}$; KH_2PO_4 0.59 $g.L^{-1}$) to limit pH
135 variations. Trace element solution was punctually added into the reactor, it was composed
136 of the following salts (mg/L): $FeCl_2$ x $4H_2O$, 2.68; H_3BO_3, 0.05; ZnCl2 x $7H_2O$, 1.01;
137 $CuCl_2$ x $2H_2O$, 0.14; $MnCl_2$ x $4H_2O$, 0.91; $H_{24}Mo_7N_6O_{24}$ x $4H_2O$, 0.09; $CoCl_2$ x $6H_2O$, 0.2;
138 $NiCl_2$ x $6H_2O$, 0.55; KI, 0.03.
139 The inoculum was composed of a mix of AD sludges from three different plants treating
140 household wastes, duck manures and bovine manures. They were pooled, centrifuged and
141 the biomass was put in suspension in a fresh minimum medium to reach an initial dry
142 weight of 2 g/L. The results presented in this study have been obtained during 405 days of
143 operation, with two shutdowns separating the experiment into three periods. The first shut
144 down happened on day 74, the culture broth was kept in the reactor under N_2 atmosphere at
145 25 ° C during 34 days. Reactor restarted on day 108 and stopped again on day 220 for 23
146 days. This time, the culture broth was stored at 4 °C.
147
148 **2.2 Gas and liquid analysis**
149 The amounts of carbon dioxide and methane in the output gas were continuously measured
150 with infrared gas analysers (X-Stream Enhanced Series, Rosemount), as well as hydrogen
151 with thermal conductivity gas analyser (Binos 100 2M, Rosemount). Gas composition was

152 also punctually analysed with a gas chromatograph (Hewlett Packard HP 5890 Series II,
153 Agilent Technologies) equipped with a HayeSep Packed column (D 100/120, 6 m length,
154 1/8 external diameter). 250 µL of sample were injected at 100 °C, argon was the carrier gas
155 at a rate of 100 mL.min^{-1}. TCD detection at 140 °C was carried out.
156 Amounts of acetate, propionate, butyrate, isobutyrate, valerate, isovalerate and hexanoate in
157 the liquid phase were measured with a gas chromatograph (VARIAN 3900 GC). The
158 column used was a CP-Wax 58 (FFAP) CB of 0.53 mm diameter and 15m length. Gas was
159 injected at 250 °C, oven temperature was 90 °C for 2 min, then increased at 130 °C at 20
160 °C.min^{-1}, after 12 min it increased again until 210 °C at 50 °C.min^{-1} and was maintained
161 during 2 min. Flame ionization detection (FID) was carried out at 240 °C.
162 Anions (F^-, Cl^-, NO_2^-, Br^-, NO_3^-, SO_4^{2-}, PO_4^{3-}) and cations (Li^+, Na^+, NH_4^+, K^+, Mg^{2+}, Ca^{2+})
163 concentrations were determined with a ionic chromatograph (Dionex™ ICS 2000, Thermo
164 Scientific™). Cation column was IonPac™ CS16 (2x250mm), eluent was methanesulfonic
165 acid 30 mM at 0.36 mL.min^{-1} and 40 °C. Anions column was IonPac™ AS19 (2x250mm),
166 eluent was KOH 20 mM, at 0.25 mL.min^{-1} and 30 °C.
167 Soluble proteins were quantified with bicinchonic acid (BCA) method (GBioscience kit).
168 Standard curve was done with bovine serum albumin (BSA) solutions from 0 to 1 gBSA.L^{-1}
169 ^{1}. Absorbance was measured in a spectrophotometer at 562 nm (Multiskan Ascent Thermo
170 Electron Corporation).
171 Nuclear Magnetic Resonance (NMR) analysis was carried out on a reactor sample of day
172 332. Broth sample was filtered (Minisart 0.2 µm syringe filter, Sartorius, Göttingen,
173 Germany). The supernatant was mixed with 100 µL of D_2O with 2.35 g L^{-1} of TSP-d4
174 (deuterated trimethylsilylpropanoic acid) as internal reference. Proton NMR spectra were

175 recorded on an Avance III 800 MHz spectrometer equipped with a 5 mM QCI-P cryo probe
176 (Bruker, Rheinstatten, Germany). Quantitative 1H-NMR was performed at 280 K, using a
177 30° pulse and a relaxation delay of 10 s. The spectra were processed and the metabolites
178 were quantified using Topspin 3.1 (Bruker, Rheinstatten, Germany).

179 **2.3 Microbiological analysis**

180 Total genomic DNA of the inoculum and some samples of the reactor was extracted with
181 FastDNA^{TM} SPIN kit for Soil (MP Biomedicals) according to the manufacturer's
182 instructions. Bacterial and archaeal 16S rRNA V4-V5 hypervariable regions were amplified
183 using the following primers: 515F-Y 5' GTGYCAGCMGCCGCGGTAA and 926R 5'
184 CCGYCAATTYMTTTRAGTTT. high-throughput sequencing was performed with S5
185 system, Ion Torrent in accordance with the manufacturer's instructions. Sequences data
186 were processed and analysed with the rANOMALY R package (Theil and Rifa, 2021). The
187 processing of raw reads in this package is based on DADA2 (Callahan et al., 2016).
188 Taxonomic assignment of bacterial and archaeal sequences was performed with IDTAXA
189 package from DECIPHER and SILVA 138 database, keeping the assignment with the
190 highest confidence or the deepest taxonomic rank. Relative abundances were obtained after
191 Total-sum normalization (TSS) of the raw ASVs counts.
192

193 **3. Results and Discussions**

194 Figure 1 shows H_2/CO_2 loads, H_2 conversion and CH_4 production (a), VFA concentrations
195 (b) and pH (c) during 405 d of operation. Two shutdowns occurred and separated periods 1,
196 periods 2 and 3. Each of these periods is discussed in the following sections regarding
197 biological methanation process performance, VFA accumulations and consumptions,

198 microbial composition and enrichment of the consortium. Figure 2 shows the CH_4
199 productivity according to H_2 loading rate during period 1 and 2, highlighting the periods
200 when instability was observed, such as the very beginning of the operation during period 1
201 and VFA accumulations during periods 2 and 3.
202 For the first time, in this study, a biological methanation reactor was operated and
203 monitored during a long-term period. The main objective in this study was to make a proof
204 of concept of the biological methanation of H_2 and CO_2 and particularly to evaluate the
205 biogas upgrading capacity for further methane injection in gas grids. The different
206 variations of inlet gas flow rates were carried out for different objectives: 1) decrease inlet
207 gas flow to increase methane purity (% CH_4 > 95 %); 2) increase gas inflow to evaluate the
208 maximal capacities of the system to convert H_2 and CO_2 into methane; 3) analyse the
209 system reactivity to these substrate load changes. In this article, the discussion is focused on
210 this third point, and on the understanding of the transient states considering microbial
211 aspects. VFA accumulations are discussed in order to understand the causes of the
212 perturbation of the process.
213
214 **3.1 Methane production and process stability during period 1**
215 **3.1.1 Process performance**
216 Period 1 was the start-up step of the process during which different gas inflows were tested,
217 starting from 0.67 to 7.78 $NL_{H2}.L^{-1}.d^{-1}$ and 0.14 to 1.73 $NL_{CO2}.L^{-1}.d^{-1}$ (Figure 2). Figure 2
218 represents the CH_4 production rates as a function of H_2 and CO_2 loading rates applied
219 during period 1 and 2. CH_4 production rates increased according to a linear correlation with
220 the loading rate, indicating that the process, especially the gas to liquid mass transfer

capacity, but also the MMC, was able to adapt to the range of gas loads applied, until 9.4 $NL.L^{-1}.d^{-1}$. Apart from the first 10 days, CH_4 productivity increased linearly with the increase of the H_2 and CO_2 loads, with average yields of 0.22 $NL_{CH4}.NL_{H2}^{-1}$ and 1.02 $NL_{CH4}.NL_{CO2}^{-1}$, representing conversions of 89 % and 102 % respectively, the stoichiometric maximal yields being 0.25 $NL_{CH4}.NL_{H2}^{-1}$ and 1 $NL_{CH4}.NL_{CO2}^{-1}$. Figure 1 shows that methanogenic activity was quickly observed during period 1 and H_2 conversion reached 83-85 % after 9 days, with a CH_4 productivity of 0.66 $NL.L^{-1}.d^{-1}$. Between 35 and 50 d, progressive increase of H_2 and CO_2 inflows from 3.6 to 4.3 and 4.8, with H_2:CO_2 ratio of 4.2, 4.6 and 4.2 respectively, resulted in instantaneous increase of CH_4 production. H_2 and CO_2 were converted at 85 ± 3 % and 107 ± 12 % respectively with a H_2/CO_2 consumed ratio of 4.8 ± 0.2 (Table 1). Between days 56 and 63, the gas loading rate was doubled instantaneously to reach 9.4 $NL.L^{-1}.d^{-1}$ at a H_2:CO_2 ratio of 4.5, closer to the calculated consumed ratio observed before. According to Figure 2, these results demonstrate that the process can rapidly reach high performances of methane production with a high conversion yield. MMC was able to adapt the conversion flux to gas load fluctuations in 4 h. A specific methane production rate of 3 $mol.gTSS^{-1}.d^{-1}$ was measured during the period between 56 and 70 d (Table 1). This adaptation capacity is crucial for methanation applications in the framework of a power-to-gas system operating with intermittent production of H_2 from renewable energies.

3.1.2 Microbial analysis

Relative abundances of the ten most represented genera in the MMC along the 405 days of experiment are presented in figure 4. During period 1, microbial analysis was performed on

244 the initial inoculum, and at days 56, 63 and 73. Composition of seeding inoculum showed
245 high diversity, with 283 OTU identified. At 56 days, only 90 OTU were identified.
246 Microbial composition remained stable from 56 to 73 d. The very drastic selection pressure
247 applied in the BCR led to a loss of diversity, and two majority genera: 58 ± 1 % of
248 *Methanobacterium* and 14 ± 2 % of *MBA03.* Genera *Lentimicrobium*, *Defluviitoga,*
249 *DTU014,* and *Coprothermobacter* represented at 5 ± 2 %, 5 ± 2 %, 2 ± 1 % and 2 ± 1 % of
250 the MMC respectively over the whole period 1. Another methanogenic genus,
251 *Methanothermobacter*, was present at 3 ± 1 %. *Methanobacterium* genus is reported as
252 hydrogenotrophic methanogenic archaea and is commonly found in biogas upgrading
253 systems at mesophilic and thermophilic temperatures (Szuhaj et al., 2021; Grimalt-
254 Alemany et al., 2019; Guneratnam et al., 2017; Luo and Angelidaki, 2012). Within this
255 group, 6.9 ± 2.1 % of *Methanobacterium formicicum* species have been identified. The
256 latter can also consume formate, acetate, propionate, butyrate, lactate, methanol, ethanol,
257 amino acids and carbohydrates to produce methane (Chellapandi et al., 2018). Although
258 metabolic function of *MBA03* is poorly understood, it is likely that it is linked to
259 carbohydrate fermentation (Jensen et al., 2021; Dyksma et al., 2020). Furthermore,
260 *Lentimicrobium* is referenced as a carbohydrate fermentative genus too. *MBA03* together
261 with *Lentimicrobium* have also been identified as potential acetate oxidizing
262 microorganisms (Zheng et al., 2019). It has been identified in numerous of AD reactors
263 especially the one treating food wastes and bovine manure, but also in biological
264 methanation reactors, at thermophilic but also mesophilic temperatures (Braga Nan et al.,
265 2020). According to the conditions in batch mode and long-term operation, it is likely that
266 *MBA03* and *Lentimicrobium* grew on lysis products, ensuring the recycling of side products

267 in the reactor. As substrates concentrations for these microorganisms (*i.e.* lysis products)
268 are low in the reactor, this could explain they are maintained at low abundance in the
269 MMC, and do not compete with autotrophs, especially methanogens. Thereby, the use of
270 MMC contributes to the stability of the operation, as side products do not accumulate in the
271 system and are substrates for heterotrophic communities. This way, the durability of the
272 process is improved, limiting the need of drains. It also increases, to a lesser extent, the
273 methane yield as the fermentation products (H_2, CO_2 and acetate) are finally transformed by
274 methanogens.
275
276 **3.2. Transient acetate and propionate accumulation and consumption during period 2**
277 **3.2.1 Volatile fatty acids producers take advantage of uncomplete methanogenesis**
278 After 34 days of shutdown, the process was started again at day 106 for the beginning of
279 period 2. Methanogenic activity was instantaneously observed, and CO_2 conversion reached
280 99 % on day 115. Gas load was increased from 2.4 to 9.6 $NL.L^{-1}.d^{-1}$ at 120 d until 140 d in
281 order to compare the performances with the same loads applied at the end of period 1 (57
282 d). This time, CH_4 production rate was no longer maximal nor stable but 50.9 ± 20.5 % and
283 32.0 ± 25.7 % between 120-134 d and 178-192 d respectively. In both periods, VFA
284 accumulated in the reactor (Figure 1), especially acetate and propionate with productivities
285 of 1.3 $mmolC.L^{-1}d^{-1}$ and 0.4 $mmolC.L^{-1}d^{-1}$ accounting for 0.7 % and 0.4 % of the H_2
286 supplied respectively between 120 and 134 d ; and productivities of 5.0 $mmolC.L^{-1}d^{-1}$ and
287 0.3 $mmolC.L^{-1}d^{-1}$ accounting for 2.9 % and 0.2 % of H_2 supplied respectively between 178
288 and 192 d. Considering this, 50-70 % of H_2 supplied was not consumed in the system
289 during these periods. This resulted in a significant increase of hydrogen partial pressure

290 (P_{H2}) and concentration in the liquid phase, a decrease in methane productivity, and a
291 decrease of pH due to VFA accumulation and CO_2 accumulation (Figure 1, Table 1). The
292 P_{H2} increase led to higher H_2 soluble concentration, and therefore a higher bioavailability of
293 the substrate for hydrogenotrophic microorganisms. This had an effect on acetate and
294 propionate productivity since hydrogen excess stimulates homoacetogenesis as it has been
295 already described in various works (Luo and Angelidaki, 2012; Agneessens et al., 2018).
296 These results also suggest that the methanogenic activity was not decreased because of
297 microbial substrate competition with VFA producers, as great amounts of H_2 substrate were
298 not consumed in the process. Here, VFA accumulation is assumed to be a consequence of a
299 lower methanogenic activity, leading to high amounts of substrate available for microbial
300 communities such as homoacetogens and other consumers of H_2 and/or CO_2.
301 Homoacetogenesis mechanism has been well described in such systems. However,
302 propionate production mechanism in chemolithoautotrophy from H_2/CO_2 remains uncertain
303 (Savvas et al., 2018; Strübing et al., 2018; Conrad and Klose, 1999). Some suggestion
304 would be that propionate production from acetyl-CoA is possible, corresponding to a
305 reductive carboxylation, operated by CODH/ACS complex involved in Wood-Ljungdahl
306 metabolic pathway (Conrad and Klose, 2000). It is also possible that some microorganisms
307 perform 3-hydroxypropionate cycle (3HPC) in which some propionyl-CoA can accumulate,
308 releasing propionate after coenzyme A regeneration. The 3HPC is known to be used by
309 some phototrophs *Chloroflexi*, as well as some hyperthermophilic archaea. Propionate can
310 also be produced from pyruvate, via lactate formation.
311 Regarding TSS measurements (Figure 3), between 107 and 133 days, average TSS
312 production was 27.3 $mg.L^{-1}.d^{-1}$ and specific methane production was 60 $mmol.gTSS^{-1}.d^{-1}$

313 while it stopped afterwards, and even decreased between 149 and 177 days. After day 177
314 the TSS production recovered to 27.7 $mg.L^{-1}.d^{-1}$ and specific methane production of 2
315 $mol.gTSS^{-1}.d^{-1}$. Therefore, the MMC, with methanogens being the majority of the
316 community, must have been nutrient limited from 133 to 177 days. The origin of
317 methanogens weakening during this period has been investigated. In order to recover the
318 methanogenic activity, productivity in CH_4 has been monitored before and after nutrient
319 injections to identify a deficiency. Various successive spikes of different nutrients such as
320 trace elements and Na_2S have been carried out. Ammonium measurements along the period
321 indicated that nitrogen was never limiting during period 2 and similar to period 1 with
322 concentration between 0.15 and 0.4 g/L which is above the limitation threshold determined
323 at 0.09 g/L for thermophilic methanogens (Rönnow and Å. H. Gunnarsson, 1982). Sulphur
324 was not measured, but the effect of supplementing the culture broth with Na_2S has been
325 studied at 133 and 192 d, and had an instantaneous effect on methanogenic activity. H_2
326 conversion yield increased to 80-85 % in both cases, and VFA concentrations decreased.
327 Here, as in previous studies, it is observed that the sulphide supply in the liquid is essential
328 for biological methanation (Figueras et al., 2021; Strübing et al., 2017). Na_2S has different
329 important functions in the system. First, it is the only sulphur source provided in the
330 mineral medium. Therefore, it is incorporated into biomass, and accounts for 0.2 – 1 %
331 ($g_S.g_{TSS}^{-1}$) (Stanbury et al., 2013). Additionally, liquid phase is almost closed, and biomass
332 is accumulating, contributing to sulphur depletion in the culture broth. During period 2, the
333 average biomass production was 11 $mg.L^{-1}.d^{-1}$. Considering biomass is composed of 1 % of
334 sulphur, the sulphur requirement in the form of Na_2S was 5.4 $mg_{Na2S}.d^{-1}$ to supply growth.
335 The initial concentration of Na_2S provided into the medium was 2 $g.L^{-1}$ which should be

enough for 373 d of growth. However, H_2S/HS^- pka is 7.04, and considering pH was around 7, but varied between 6 and 8, the sulphur added in the medium was mainly in the forms of HS^- and H_2S. Although it was not measured, it is assumed that H_2S stripping was significant considering the gas phase was open. Na_2S is also a strong reducing agent, contributing, with H_2, to maintain low ORP in the medium. Chemical or biological sulphide oxidation also allows to consume traces of oxygen in the reactor, that would be toxic for methanogens. Finally, a source of sulphur loss is the output of liquid. Although the retention time is very high (> 130 d), some culture broth extraction was operated to maintain the volume constant during long term operations. This also contributed to the elimination of nutrients in the medium as it was replaced with bicarbonate solution. Further investigations on sulphur supply and sulphide functions is necessary to be able to control correctly the process regarding Na_2S supply.

3.2.2 Microbial analysis

During period 2, microbial composition of the consortium was similar to period 1 (Figure 4). *Methanobacterium* was the dominant genus, followed with minority bacterial genera such as *Lentimicrobium*, *MBA03*, *DTU014* and *Coprothermobacter*. However, the particularity of period 2 compared to period 1 is the significant abundance of genus *Tepidiphilus* of 2.2-13.7 %, and the decreasing abundance of *MBA03* between 126 and 147 d. MMC composition finally recovered a similar profile to period 1 between 192 and 219 d, except that *Coprothermobacter* became more abundant and *Lentimicrobium* less abundant. *Tepidiphilus* genus belongs to proteobacteria, it is mostly thermophilic. These microorganisms can use hydrogen or inorganic sulphur compounds as electron donor for

chemotrophic growth, as well as acetate for heterotrophic growth (Manaia et al., 2003). This genus increased in the consortium when acetate was produced, and it is likely that acetate was accumulated because of a lack of *MBA03* for its oxidation. *MBA03* has been found to be associated to trace element supplementation in an AD reactor (FitzGerald et al., 2019). Its disappearance between 126 and 147 d might be linked to a trace element limitation. Trace elements were supplied at 180 d, and MBA03 increased again in the consortium from this day according to Figure 4. *Tepidiphilus* as well as *Coprothermobacter* have been found to dominate a MMC in a bioelectrochemical system converting acetate into power (Dessì et al., 2019). This is consistent with the accumulation of acetate observed during period 2. During this transitory state, *Tepidiphilus* and *Coprothermobacter* took advantage of acetate production to carry out acetate oxidation. Genus *Tepidanaerobacter* was also present at 1-4 % in the MMC between 147 and 192 d, and it is known to perform SAO. Acetogens have a highly versatile metabolism and most of them can switch from heterotrophic to autotrophic growth depending on substrate availability and environmental conditions (Batstone et al., 2002). According to Figure 4, the abundances of *Tepidiphilus*, *Tepidimicrobium* and *Lentimicrobium* in the MMC increased during the VFA accumulating period, indicating that they could be linked to acetate and propionate production, as well as their consumption depending on the environmental conditions. Especially, gas partial pressures can reverse the thermodynamic feasibility of the reactions in favour of VFA production when they are high, or VFA oxidation if they are low.

3.3. Four and five carbons organic acids accumulation during period 3

3.3.1 Proteolysis or chain elongation?

382 Period 3 corresponds to an intensification of the process. Effective volume was decreased
383 from 20 L to 18 L, small diffusers were changed for a full column bottom area diffuser,
384 enabling to increase gas supply until 18 $NL.L^{-1}.d^{-1}$ (Figure 1). Higher methane
385 concentration up to 90 % in the outlet gas was achieved. However, other organic acids
386 beside acetate and propionate were detected with gas chromatograph (GC) such as butyrate,
387 isobutyrate and isovalerate (Figure 1). Propionate accumulated until 290 d and then,
388 between 291 d and 301 d, propionate concentration decreased from 0.65 to 0.30 $g.L^{-1}$
389 corresponding to $4.7.10^{-3}$ mol consumed and C5 organic acids increased from 0.25 to 0.63
390 $g.L^{-1}$ corresponding to $3.7.10^{-3}$ mol produced. Simultaneously to C5 organic acids
391 accumulation, a decrease of propionate concentration was observed. This co-occurrence
392 suggests that odd carbon chain elongation could be active. Chain elongation corresponds to
393 reverse β-oxidation cycles, allowing lengthening of the carbon chain with two carbon atoms
394 by creation of C-C bond. The mechanism has been described in *C. kluyveri* (Seedorf et al.,
395 2008). Coma et al. (2016) showed by thermodynamic calculations that different
396 alcohol/carboxylate combinations were favourable for chain elongation, which explains the
397 synthesis of odd carboxylates in some cases (El-Gammal et al., 2017). In particular,
398 heptanoate could be obtained from ethanol and propionate, with valerate as intermediate
399 (Grootscholten et al., 2013). Odd-numbered carboxylates such as valerate are interesting
400 because they can be used for the production of PHA-type polymers with different
401 properties from those conferred by even-numbered carboxylates.
402 In the other side, NMR analysis at day 332 revealed the presence of 2-methylbutyrate,
403 which in fact, was the majority C5 organic acid. 2-methylbutyrate, isobutyrate and
404 isovalerate are branched chain organic acids. This VFA mixture must rather come from

amino acids fermentation (Stickland reactions). It is known that peptides and amino acids fermentation releases acetate, propionate, butyrate, valerate, isobutyrate, isovalerate, 2-methylbutyrate, aromatic compounds such as phenylacetate, phenylpropionate, inorganic carbon, ammonia and reduced sulphur (McInerney and Bryant, 1981). Proteins have been quantified in the soluble fraction of the culture medium (Figure 3). Proteins concentration did not vary to a great extend during period 2 while it did during period 3. Indeed, proteins were continuously released with a rate of 5.7 ± 0.3 mg(eq-BSA).L^{-1}.d^{-1}. 2-methylbutyrate and isovalerate can be obtained after deamination and decarboxylation of isoleucine and leucine respectively (Girbal et al., 1997). These last amino acids are the most hydrophobic ones involved in proteins constitution also with valine. They are thus highly represented in cell membranes proteins (Kaneda, 1991). It is possible those proteins detected in the medium come from cell decay, and that some heterotrophs grow on the lysis products, especially proteolytic microorganisms. This is consistent with the reactor running with a closed liquid mode, allowing cell death and recycling in the culture broth. As process activity has been intensified during period 3, death and matter recycling in the process could be observed while they were too low in the previous periods.

3.3.2 Microbial analysis of period 3

During period 3, The dominant genus was still *Methanobacterium* until 372 d. At this point, the methanogenic community changed and genus *Methanothermobacter* took the advantage, representing progressively 50 % of the consortium at day 405 while *Methanobacterium* was only 2 %. Another interesting observation is that *Coprothermobacter* genus was more represented in the consortium compared to periods 1

and 2, accounting for 10-15 % of relative abundance (Figure 4). Conversely to *Methanobacterium*, *Methanothermobacter* is found in thermophilic systems only, some of the strains can use formate, but the others are obligate autotrophs. Daily drains were applied from day 364, implying a lower hydraulic retention time of 71 d. This could explain the switch in methanogenic community from *Methanobacterium* to *Methanothermobacter*, although, this high retention tim corresponds to a dilution rate of 0.014 d, which is lower than the maximal specific growth rates reported for thermophilic hydrogenotrophic methanogens (0.02 – 12 d^{-1}) (Batstone et al., 2002). Szuhaj et al. (2021) observed that *Methanobacterium* abundance decreased with the H_2 supply increasing, while *Methanothermobacter* had a reverse behaviour. The intensification of the process, with higher gas supply could also explain the selection of *Methanothermobacter* along period 3 and demonstrates the competition between the two genera according to H_2 supply. *Coprothermobacter spp.* are known as thermophilic and proteolytic microorganisms, commonly found in anaerobic environment, especially AD reactors (Braga Nan et al., 2020; Grimalt-Alemany et al., 2019; Zheng et al., 2019). Proteolytic activity of such anaerobes produces acetate, H_2 and CO_2, as well as few isobutyrate, isovalerate and propionate. As discussed previously, this VFA mixture profile is consistent with the VFA detected in the biological methanation reactor. Proteolysis is also accompanied with inorganic nitrogen and carbon release due to deamination and decarboxylation of amino acids respectively. This could explain that the calculated ratio of H_2/CO_2 consumed is higher than the one of the sole methanogenesis reaction (*i.e.* 4) because some CO_2 can be produced along fermentation processes. *Coprothermobacter spp.* produce high concentrations of intracellular and extracellular proteases. Thus, it is possible that the proteins concentration

451 measured in the supernatant were hydrolytic enzymes such as proteases. Considering this, it
452 is likely that the second hypothesis about the origin of the branched chain C4 and C5
453 carboxylates found in period 3 is confirmed, these molecules might be produced from lysis
454 products and proteolytic activity, consuming dead cells. As period 3 was an intensification
455 phase of the study, higher biomass concentrations were reached, implying higher death rate
456 as well, and this could explain that the concentrations of VFA increased during this period.
457 Furthermore, syntrophic relationships have been previously highlithed between
458 *Coprothermobacter* and *Methanothermobacter* in AD reactors (Gagliano et al., 2015;
459 Zheng et al., 2019). Grimalt-Alemany et al. (2019) also identified *Coprothermobacter* and
460 *Methanothermobacter* as majority genera in their thermophilic enrichments of MMC for
461 biological methanation of syngas. Here, in the *ex situ* biological methanation of H_2/CO_2,
462 hydrogenotrophic methanogens are the most represented microorganisms in the consortium,
463 it is likely that soluble hydrogen concentration is close to zero due to methanogenic
464 activity, enhancing proteolytic activity.
465
466 **3.4. Effect of starvation periods on microbial composition and reactor performances**
467 The reactor was stopped during 34 days between 72 and 106 d, with the culture broth kept
468 inside at room temperature. During this starvation period, microbial relative composition
469 changed (Figure 4). While *Methanobacterium* represented 59 % of the consortium before
470 the shutdown, it did only 26 % afterward. Conversely, *Lentimicrobium* relative abundance
471 increased from 3 % to 12 % before and after the shutdown respectively. However,
472 methanogenic activity recovered to 83 % H_2 and 69 % CO_2 conversion rates in less than
473 24 h, and 91 % H_2 and 86 % CO_2 after 8 days, indicating that methanogenic activity was

474 resilient to the storage conditions and capable of a fast reactivation (Figure 1). Furthermore,
475 as discussed in previous sections, MMC composition moved toward the same profile as in
476 period 1 when nutrient limitations were overcome, demonstrating the reproducibility of the
477 MMC enrichment in these conditions. During the starvation period at room temperature,
478 some communities of *Proteobacteria* and *Bacteroidetes* phyla could have grown
479 heterotrophically, probably on lysis products, increasing their relative abundance.
480 Hydrogenotrophic methanogenic archaea probably did not grow during this storage period
481 because of the lack of H_2/CO_2, but were able to restart quickly, despite their relative
482 abundance decreased, which suggests they maintained themselves in a non-growing or very
483 slow growing state. Indeed, it has been shown that restart performances after a storage
484 period was better for a storage temperature of 25 °C than 55 °C, due to lower inactivation
485 rate at room temperature than thermophilic temperature (Strübing et al., 2019). The next
486 storage period was carried out at 4 °C for 23 days between periods 2 and 3 (Figure 1).
487 According to Figure 4, MMC composition was maintained with similar relative abundances
488 of the different genera found at the end of period 2. This was expected as low temperatures
489 stop biological activity and stabilize the MMC. In this case the activity recovered to 93 %
490 H_2 and 85 % CO_2 conversions within 3 days, suggesting that storage at 4 °C also allowed a
491 fast recovery of performances of the MMC for methane production. However, the
492 performances obtained after 3 days in case of a storage at 4 °C during 23 d were
493 comparable to the performances obtained after 8 days in the case of storage at room
494 temperature during 34 d. The storage of the MMC at 4°C during 23 d therefore allowed a
495 better preservation of the activity, however, on a large scale, it is more complicated, and
496 costly in terms of energy, to implement this low temperature storage. This is consistent

with the fact that genus *Methanobacterium* turns out to be more resistant to high hydrogen partial pressures, VFA accumulation, and starvation period. Braga et al. (2022) showed that *Methanobacterium* was capable of recovering a methanogenic activity within a week after a starvation period of four weeks, outcompeting other methanogens in presence before the starvation period, indicating the high potential of these microbes for the development of biological methanation at large scale.

4. Conclusion

In this study of an *ex situ* biological methanation system with MMC during 405d, productivity of $4N.L^{-1}.d^{-1}$ of CH_4 was obtained with up to 94% of H_2/CO_2 conversion. VFA accumulations was observed as a consequence of the methanogens limited growth. Methanogens were mostly represented by *Methanobacterium* genus during the first stage of operation, and *Methanothermobacter* after intensification of the process. MMC was resilient to storage periods of 34d and 23d at room temperature and 4°C respectively indicating its suitability for large scale and long-term operations.

Acknowledgements

This research was supported by the french National Institute of Applied Sciences (INSA) of Toulouse, the French National Institute for Agricultural Research (INRAE), and funded by the French agency for ecological transition (ADEME), and the french Occitanie region. The Bioenergies, Biomolecules, Biomaterials, renewable carbon recovery (3BCAR) for financial support in the framework of the project FullForBest(16S rRNA sequencing). The authors want to gratefully acknowledge Evrard Mengelle for his technical support, Mansour

Bounouba for his analytical support, Fabien Létisse for NMR analysis, Viviana Contreras from ENOSIS for her experimental contribution, the platform Get Biopuces for high throughput sequencing and metagenomic analysis, Myriam Mercade and pascale Lepercq from TBI for DNA extraction training.

Data availability

Raw sequences were submitted to NCBI Sequence Read Archive (SRA) database and are available under the BioProject ID PRJNA821448 (BioSample accessions SAMN27097652-SAMN27097680).

References

1. Agneessens, L.M., Ottosen, L.D.M., Andersen, M., Berg Olesen, C., Feilberg, A., Kofoed, M.V.W., 2018. Parameters affecting acetate concentrations during in-situ biological hydrogen methanation. Bioresour. Technol. 258, 33–40.
2. Angelidaki, I., Treu, L., Tsapekos, P., Luo, G., Campanaro, S., Wenzel, H., Kougias, P.G., 2018. Biogas upgrading and utilization: Current status and perspectives. Biotechnol. Adv. 36, 452–466.
3. Bassani, I., Kougias, P.G., Treu, L., Angelidaki, I., 2015. Biogas Upgrading via Hydrogenotrophic Methanogenesis in Two-Stage Continuous Stirred Tank Reactors at Mesophilic and Thermophilic Conditions. Environ. Sci. Technol. 49, 20, 12585–12593
4. Batstone, D.J., Keller, J., Angelidaki, I., Kalyuzhnyi, S.V., Pavlostathis, S.G., Rozzi, A., Sanders, W.T.M., Siegrist, H., Vavilin, V.A., 2002. The IWA Anaerobic Digestion Model No 1 (ADM1). Water Sci. Technol. 45, 65–73.
5. Braga Nan, L., Trably, E., Santa-Catalina, G., Bernet, N., Delgenes, J.-P., Escudie, R., 2022. Microbial community redundance in biomethanation systems lead to faster recovery of methane production rates after starvation. Sci. Total Environ. 804, 150073.
6. Braga Nan, L., Trably, E., Santa-Catalina, G., Bernet, N., Delgenès, J.-P., Escudié, R., 2020. Biomethanation processes: new insights on the effect of a high H2 partial pressure on microbial communities. Biotechnol. Biofuels 13, 141.
7. Burkhardt, M., Koschack, T., Busch, G., 2015. Biocatalytic methanation of hydrogen and carbon dioxide in an anaerobic three-phase system. Bioresour. Technol. 178, 330–333.

8. Callahan, B.J., McMurdie, P.J., Rosen, M.J., Han, A.W., Johnson, A.J.A., Holmes, S.P., 2016. DADA2: High-resolution sample inference from Illumina amplicon data. Nat. Methods 13, 581–583.
9. Campanaro, S., Treu, L., Rodriguez-R, L.M., Kovalovszki, A., Ziels, R.M., Maus, I., Zhu, X., Kougias, P.G., Basile, A., Luo, G., Schlüter, A., Konstantinidis, K.T., Angelidaki, I., 2020. New insights from the biogas microbiome by comprehensive genome-resolved metagenomics of nearly 1600 species originating from multiple anaerobic digesters. Biotechnol. Biofuels 13, 25.
10. Chellapandi, P., Bharathi, M., Sangavai, C., Prathiviraj, R., 2018. Methanobacterium formicicum as a target rumen methanogen for the development of new methane mitigation interventions: A review. Vet. Anim. Sci. 6, 86–94.
11. Coma, M., Vilchez-Vargas, R., Roume, H., Jauregui, R., Pieper, D.H., Rabaey, K., 2016. Product Diversity Linked to Substrate Usage in Chain Elongation by Mixed-Culture Fermentation. Environ. Sci. Technol. 50, 6467–6476.
12. Conrad, R., Klose, M., 2000. Selective inhibition of reactions involved in methanogenesis and fatty acid production on rice roots. FEMS Microbiol. Ecol. 34, 27–34.
13. Conrad, R., Klose, M., 1999. Anaerobic conversion of carbon dioxide to methane, acetate and propionate on washed rice roots. FEMS Microbiol. Ecol. 30, 147–155.
14. Cord-Ruwisch, R., Seitz, H.-J., Conrad, R., 1988. The capacity of hydrogenotrophic anaerobic bacteria to compete for traces of hydrogen depends on the redox potential of the terminal electron acceptor. Arch. Microbiol. 149, 350–357.
15. Dessì, P., Chatterjee, P., Mills, S., Kokko, M., Lakaniemi, A.-M., Collins, G., Lens, P.N.L., 2019. Power production and microbial community composition in thermophilic acetate-fed up-flow and flow-through microbial fuel cells. Bioresour. Technol. 294, 122115.
16. Drosg, B., 2013. Process monitoring in biogas plants. IEA Bioenergy 38.
17. Dyksma, S., Jansen, L., Gallert, C., 2020. Syntrophic acetate oxidation replaces acetoclastic methanogenesis during thermophilic digestion of biowaste. Microbiome 8, 105.
18. El-Gammal, M., Abou-Shanab, R., Angelidaki, I., Omar, B., Sveding, P.V., Karakashev, D.B., Zhang, Y., 2017. High efficient ethanol and VFA production from gas fermentation: Effect of acetate, gas and inoculum microbial composition. Biomass Bioenergy 105, 32–40.
19. Figueras, J., Benbelkacem, H., Dumas, C., Buffière, P., 2021. Biomethanation of syngas by enriched mixed anaerobic consortium in pressurized agitated column. Bioresour. Technol. 338.
20. FitzGerald, J.A., Wall, D.M., Jackson, S.A., Murphy, J.D., Dobson, A.D.W., 2019. Trace element supplementation is associated with increases in fermenting bacteria in biogas mono-digestion of grass silage. Renew. Energy 138, 980–986.
21. Gagliano, M.C., Braguglia, C.M., Petruccioli, M., Rossetti, S., 2015. Ecology and biotechnological potential of the thermophilic fermentative Coprothermobacter spp. FEMS Microbiol. Ecol. 91.

22. Girbal, L., Örlygsson, J., Reinders, B.J., Gottschal, J.C., 1997. Why Does Clostridium acetireducens Not Use Interspecies Hydrogen Transfer for Growth on Leucine? Curr. Microbiol. 35, 155–160.
23. González-Cabaleiro, R., Lema, J.M., Rodríguez, J., Kleerebezem, R., 2013. Linking thermodynamics and kinetics to assess pathway reversibility in anaerobic bioprocesses. Energy Environ. Sci. 6, 3780–3789.
24. Grimalt-Alemany, A., Łężyk, M., Kennes-Veiga, D.M., Skiadas, I.V., Gavala, H.N., 2019. Enrichment of Mesophilic and Thermophilic Mixed Microbial Consortia for Syngas Biomethanation: The Role of Kinetic and Thermodynamic Competition. Waste Biomass Valor. 11, 465–481.
25. Grootscholten, T.I.M., Steinbusch, K.J.J., Hamelers, H.V.M., Buisman, C.J.N., 2013. High rate heptanoate production from propionate and ethanol using chain elongation. Bioresour. Technol. 136, 715–718.
26. Guneratnam, A.J., Ahern, E., FitzGerald, J.A., Jackson, S.A., Xia, A., Dobson, A.D.W., Murphy, J.D., 2017. Study of the performance of a thermophilic biological methanation system. Bioresour. Technol. 225, 308–315.
27. Jensen, M.B., de Jonge, N., Dolriis, M.D., Kragelund, C., Fischer, C.H., Eskesen, M.R., Noer, K., Møller, H.B., Ottosen, L.D.M., Nielsen, J.L., Kofoed, M.V.W., 2021. Cellulolytic and Xylanolytic Microbial Communities Associated With Lignocellulose-Rich Wheat Straw Degradation in Anaerobic Digestion. Front. Microbiol. 12, 1148.
28. Kaneda, T., 1991. Iso- and anteiso-fatty acids in bacteria: biosynthesis, function, and taxonomic significance. Microbiol. Mol. Biol. Rev. 55, 288–302.
29. Kougias, P.G., Treu, L., Benavente, D.P., Boe, K., Campanaro, S., Angelidaki, I., 2017. Ex-situ biogas upgrading and enhancement in different reactor systems. Bioresour. Technol. 225, 429–437.
30. Luo, G., Angelidaki, I., 2012. Integrated biogas upgrading and hydrogen utilization in an anaerobic reactor containing enriched hydrogenotrophic methanogenic culture. Biotechnol. Bioeng. 109, 2729–2736.
31. Manaia, C.M., Nogales, B., Nunes, O.C.Y. 2003, 2003. Tepidiphilus margaritifer gen. nov., sp. nov., isolated from a thermophilic aerobic digester. Int. J. Syst. Evol. Microbiol. 53, 1405–1410.
32. McCarty, P.L., Bae, J., 2011. Model to Couple Anaerobic Process Kinetics with Biological Growth Equilibrium Thermodynamics. Environ. Sci. Technol. 45, 6838–6844.
33. McInerney, M.J., Bryant, M.P., 1981. Basic Principles of Bioconversions in Anaerobic Digestion and Methanogenesis, in: Sofer, S.S., Zaborsky, O.R. (Eds.), Biomass Conversion Processes for Energy and Fuels. Springer US, Boston, MA, pp. 277–296.
34. Pan, X., Zhao, L., Li, C., Angelidaki, I., Lv, N., Ning, J., Cai, G., Zhu, G., 2021. Deep insights into the network of acetate metabolism in anaerobic digestion: focusing on syntrophic acetate oxidation and homoacetogenesis. Water Res. 190, 116774.
35. Rafrafi, Y., Laguillaumie, L., Dumas, C., 2020. Biological Methanation of H2 and CO2 with Mixed Cultures: Current Advances, Hurdles and Challenges. Waste Biomass Valor. 12, 5259–5282.

642 36. Rönnow, P.H., Å. H. Gunnarsson, L., 1982. Response of growth and methane
643 production to limiting amounts of sulfide and ammonia in two thermophilic
644 methanogenic bacteria. FEMS Microbiol. Lett. 14, 311–315.
645 37. Savvas, S., Donnelly, J., Patterson, T., Chong, Z.S., Esteves, S.R., 2018. Methanogenic
646 capacity and robustness of hydrogenotrophic cultures based on closed nutrient
647 recycling via microbial catabolism: Impact of temperature and microbial
648 attachment. Bioresour. Technol. 257, 164–171.
649 38. Seedorf, H., Fricke, W.F., Veith, B., Brüggemann, H., Liesegang, H., Strittmatter, A.,
650 Miethke, M., Buckel, W., Hinderberger, J., Li, F., Hagemeier, C., Thauer, R.K.,
651 Gottschalk, G., 2008. The genome of Clostridium kluyveri, a strict anaerobe with
652 unique metabolic features. Proc. Natl. Acad. Sci. 105, 2128–2133.
653 39. Stanbury, P.F., Whitaker, A., Hall, S.J., 2013. Principles of Fermentation Technology,
654 Pergamon 2nd ed. Elsevier Science Ltd, Oxford.
655 40. Strübing, D., Huber, B., Lebuhn, M., Drewes, J.E., Koch, K., 2017. High performance
656 biological methanation in a thermophilic anaerobic trickle bed reactor. Bioresour.
657 Technol. 245, 1176–1183.
658 41. Strübing, D., Moeller, A.B., Mößnang, B., Lebuhn, M., Drewes, J.E., Koch, K., 2019.
659 Load change capability of an anaerobic thermophilic trickle bed reactor for dynamic
660 H2/CO2 biomethanation. Bioresour. Technol. 289, 121735.
661 42. Strübing, D., Moeller, A.B., Mößnang, B., Lebuhn, M., Drewes, J.E., Koch, K., 2018.
662 Anaerobic thermophilic trickle bed reactor as a promising technology for flexible
663 and demand-oriented H2/CO2 biomethanation. Appl. Energy 232, 543–554.
664 43. Szuhaj, M., Wirth, R., Bagi, Z., Maróti, G., Rákhely, G., Kovács, K.L., 2021.
665 Development of Stable Mixed Microbiota for High Yield Power to Methane
666 Conversion. Energies 14, 7336.
667 44. Theil, S., Rifa, E., 2021. rANOMALY: AmplicoN wOrkflow for Microbial community
668 AnaLYsis. F1000Research 10, 7. https://doi.org/10.12688/f1000research.27268.1
669 45. Weijma, J., Gubbels, F., Hulshoff Pol, L.W., Stams, A.J.M., Lens, P., Lettinga, G.,
670 2002. Competition for H2 between sulfate reducers, methanogens and
671 homoacetogens in a gas-lift reactor. Water Sci. Technol. 45, 75–80.
672 46. Zheng, D., Wang, H.-Z., Gou, M., Nobu, M.K., Narihiro, T., Hu, B., Nie, Y., Tang, Y.-
673 Q., 2019. Identification of novel potential acetate-oxidizing bacteria in thermophilic
674 methanogenic chemostats by DNA stable isotope probing. Appl. Microbiol.
675 Biotechnol. 103, 8631–8645.
676

677 **Figure captions**

678 Table 1: Performances of the thermophilic *ex situ* biological methanation along the

679 different periods of operation.

680

Figure 1: (a) H_2 inflow in $NL.L^{-1}.d^{-1}$ (red line), CO_2 inflow in $NL.L^{-1}.d^{-1}$ (blue line), CH_4 outflow in $NL.L^{-1}.d^{-1}$ (orange squares) and H_2 conversion in % (black circles) ; (b) Volatile fatty acid concentrations: C2 mainly composed of acetate (square), C3 mainly composed of propionate (triangle), C4 mainly composed of butyrate (yellow circle), iC4 mainly composed of isobutyrate (orange circle) and iC5 composed of a mixture of isomers isovalerate and 2-methylbutyrate (blue circle), arrows show supernatant have been drained three times and replaced by carbonate solution, half of the supernatant at 303 d and a quarter at 352 d and again half of the supernatant at 373 d. A 250 mL daily drain has been implemented from day 364 (grey area); (c) pH evolution.

Figure 2: CH_4 productivity as a function of H_2 (top) and CO_2 (below) loading rates during period 1 and period 2. Green circles represent stable periods of the process. In red the periods of instability: start-up of the operation during period 1 from 0 to 10 d (squares), and VFA accumulation during period 2 from 120 to 140 d (triangles) and from 176 to 193 d (squares).

Figure 3: Soluble proteins concentration in g(eq-BSA)/L (blue squares) and TSS concentration in g/L (yellow circles) in the culture broth along the experiment. Dot lines represent the starvation periods.

Figure 4: Relative abundance of the ten most represented genera in the MMC along the experiment obtained with rANOMALY pipeline (Theil and Rifa, 2021).

Tables and Figures

	d	Inflow H_2/CO_2 ratio	Consumed H_2/CO_2 ratio	% H_2 conversion	%CO_2 conversion	Specific CH_4 production ($mol.gTSS^{-1}.d^{-1}$)	Average Volumic CH_4 production ($NL_{CH4}.L^{-1}.d^{-1}$
Period 1	0-10	4.0 ± 0.0	4.5 ± 5.9	45 ± 39	44 ± 35	-	-
	15-35	5.8 ± 2.1	6.6 ± 3.6	88 ± 7	125 ± 48	-	0.45 ± 0.23
	36-55	4.6 ± 0.1	4.8 ± 0.2	85 ± 3	107 ± 12	-	0.85 ± 0.10
	56-63	4.5 ± 0.0	4.4 ± 0.1	74 ± 6	103 ± 12	3	1.67 ± 0.30
	64-70	5.4 ± 1.4	5.6 ± 1.5	93 ± 4	96 ± 41		0.44 ± 0.25
Period 2	107-119	5.3 ± 1.7	5.3 ± 1.8	86 ± 7	87 ± 13	2	0.85 ± 0.50
	120-164	4.6 ± 0.0	5.1 ± 0.6	79 ± 19	72 ± 18	-	1.08 ± 0.46
	165-205	4.0 ± 0.0	5.8 ± 2.4	65 ± 24	51 ± 27	2	1.27 ± 0.46
Period 3	242-405	4.2 ± 0.1	4.2 ± 3.9	94 ± 10	94 ± 24	1	3.97 ± 3.04

Table 1: Performances of the thermophilic *ex situ* biological methanation along the different periods of operation.

Colour print is not needed

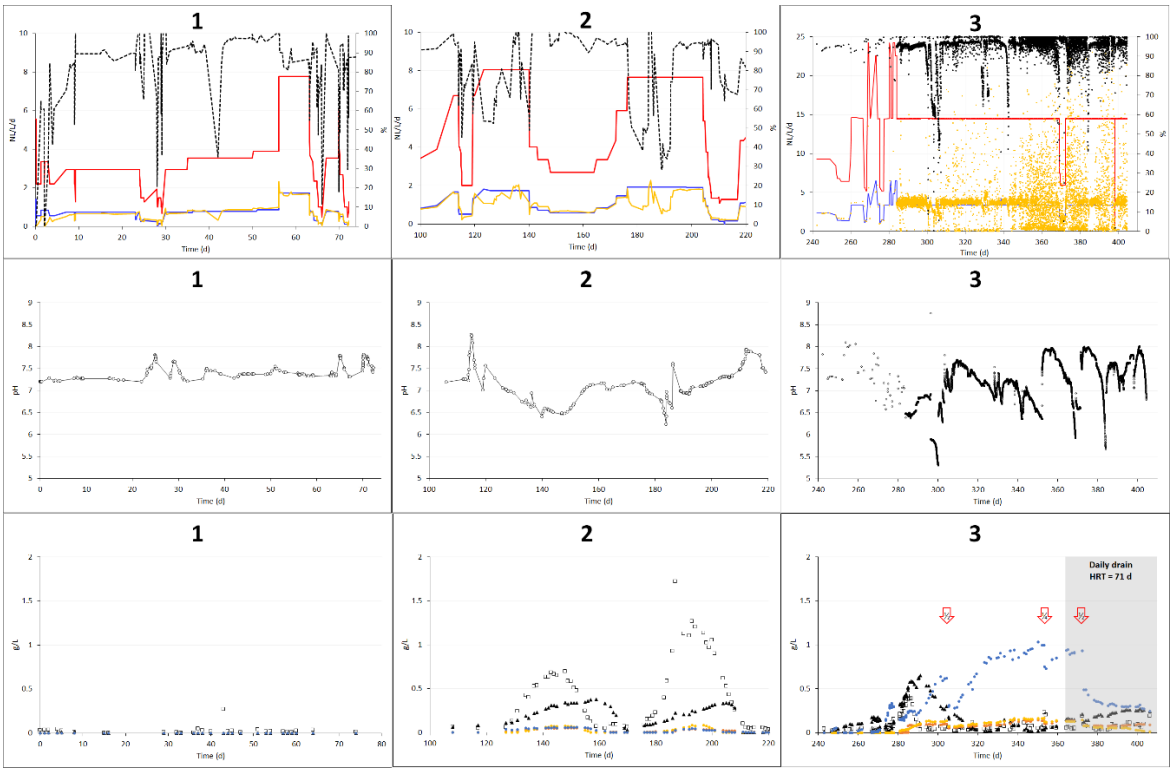

Figure 1: (a) H_2 inflow in $NL.L^{-1}.d^{-1}$ (red line), CO_2 inflow in $NL.L^{-1}.d^{-1}$ (blue line), CH_4 outflow in $NL.L^{-1}.d^{-1}$ (orange squares) and H_2 conversion in % (black circles) ; (b) Volatile fatty acid concentrations: C2 mainly composed of acetate (square), C3 mainly composed of propionate (triangle), C4 mainly composed of butyrate (yellow circle), iC4 mainly composed of isobutyrate (orange circle) and iC5 composed of a mixture of isomers isovalerate and 2-methylbutyrate (blue circle), arrows show supernatant have been drained three times and replaced by carbonate solution, half of the supernatant at 303 d and a quarter at 352 d and again half of the supernatant at 373 d. A 250 mL daily drain has been implemented from day 364 (grey area); (c) pH evolution.

Colour print is needed

High quality file has been provided separately

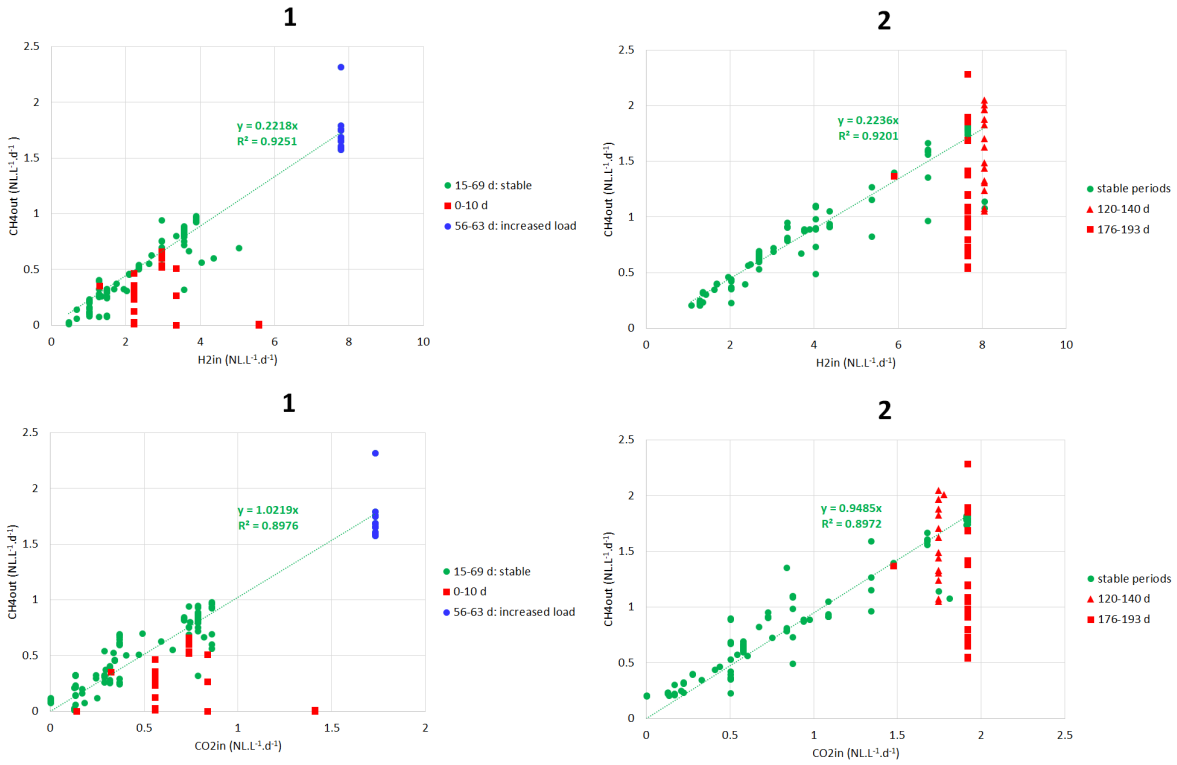

Figure 2: CH_4 productivity as a function of H_2 (top) and CO_2 (below) loading rates during period 1 and period 2. Green circles represent stable periods of the process. In red the periods of instability: start-up of the operation during period 1 from 0 to 10 d (squares), and VFA accumulation during period 2 from 120 to 140 d (triangles) and from 176 to 193 d (squares).

Colour print is needed

High quality file has been provided separately

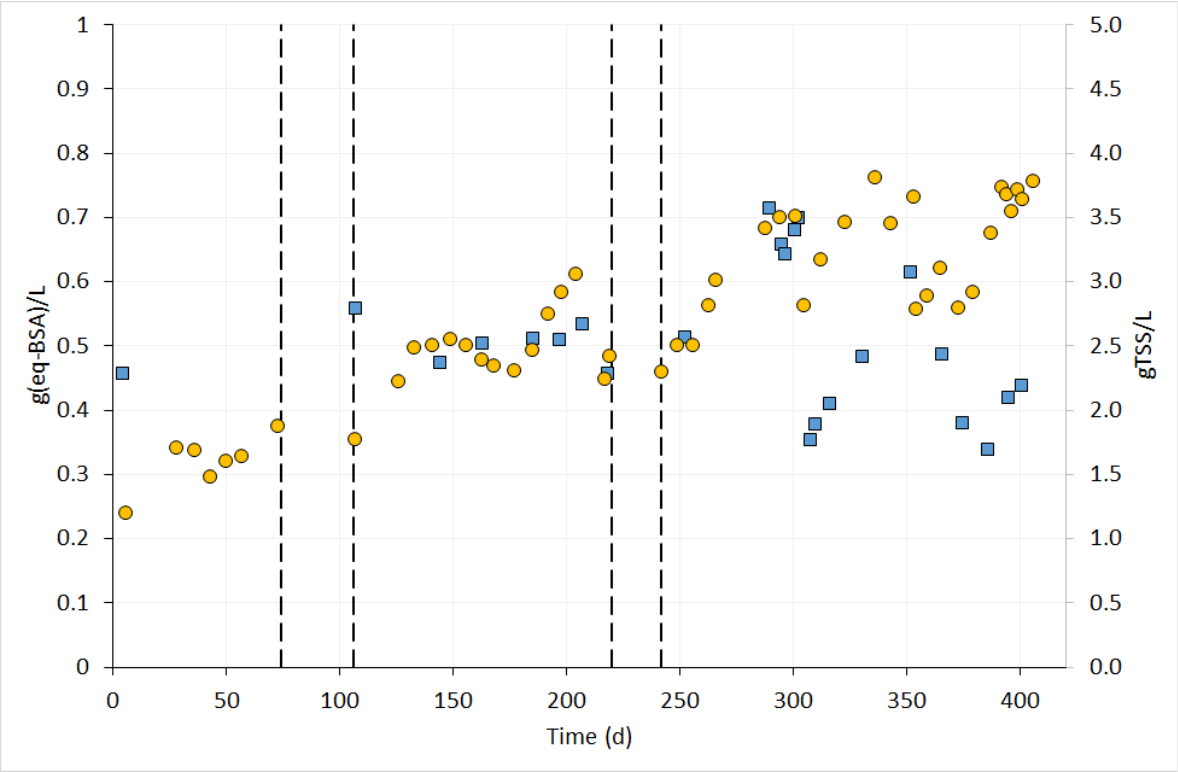

Figure 3: Soluble proteins concentration in g(eq-BSA)/L (blue squares) and TSS concentration in g/L (yellow circles) in the culture broth along the experiment. Dot lines represent the starvation periods.

Colour print is needed

High quality file has been provided separately

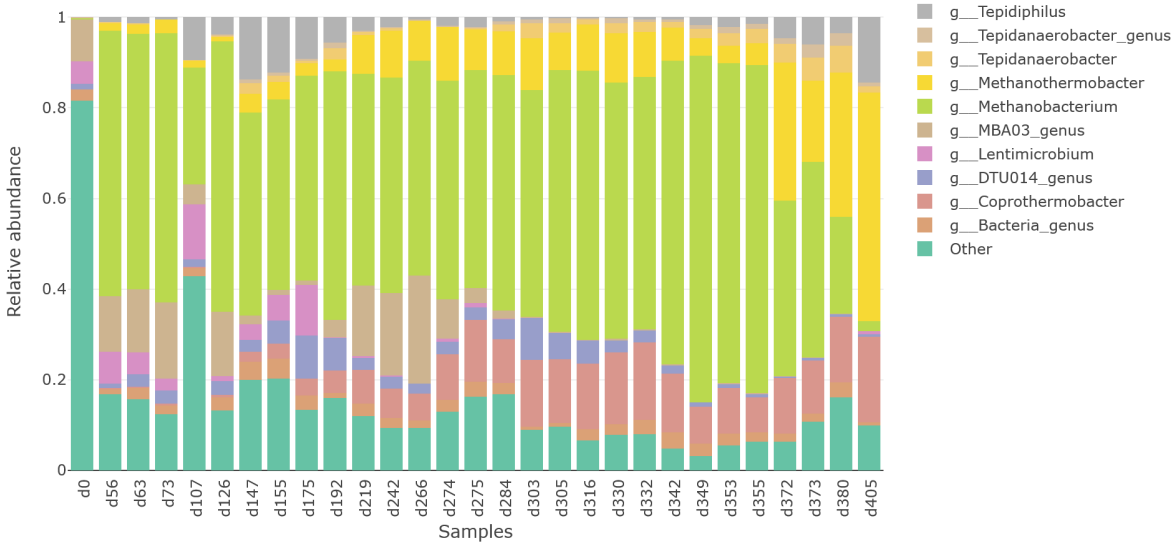

Figure 4: Relative abundance of the ten most represented genera in the MMC along the experiment obtained with rANOMALY pipeline (Theil and Rifa, 2021).

Colour print is needed

High quality file has been provided separately